Amplified Spontaneous Green Emission and Lasing Emission From Carbon Nanoparticles

Songnan Qu, Xingyuan Liu, Xiaoyang Guo, Minghui Chu, Ligong Zhang, and Dezhen Shen**

In this work, the optical properties of carbon nanoparticles (CNPs) can be modulated by the dopant-N atom and sp^2 C-contents. CNPs prepared with the low urea mass ratio of 0.2:1 (CNP1) exhibit blue emission (maximum PL quantum yield: 15%). Increasing sp^2 C- and dopant-N atom contents, as determined in CNPs prepared with high urea mass ratio of 2:1 (CNP2), lead to green emission (maximum PL quantum yield up to 36% in ethanol aqueous solution). Amplified spontaneous emission (ASE) can be observed only in CNP2 ethanol aqueous solution. Green lasing emission is achieved from CNP2 ethanol aqueous solution in a linear long Fabry-Perot cavity, indicating the potential of CNP2 as a gain medium for lasing. CNP2 shows superior photostability compared with C545T dye. The green emission from CNP2 is speculated to arise from electron-hole recombination (intrinsic state emission). The high PL quantum yield and small overlap between absorption and emissions of CNP2 ethanol aqueous solution are the key factors in realizing lasing emission.

1. Introduction

Carbon is an important and popular material, which is hardly considered as a member of the "luminescent material familly". However, it was found unambiguously that nanoscale carbon particles could exhibit brightly fluorescence.[1] Much attention have been paid on the emerging luminescent carbon-nanoparticles (CNPs) not only because of their superior properties, such as low cost, chemical inertness, lack of optical blinking, low photobleaching, low cytotoxicity, excellent biocompatible and attracting potential applications,[2–5] but also because the luminescence mechanism of CNPs is still not clearly understood. Lasing emission is a very important research content of luminescent materials. Realizing lasing emission from CNPs is a breakthrough of carbon materials. Yu et al. have done pioneer work in producing lasing emissions in deep blue region from CNPs organic solvents in high-Q cylindrical microcavities by coating polyethylene glycol (PEG 200) with modified CNPs onto the surface of optical fibers.[6a] Random lasing action in deep blue region was also observed from graphene nanoparticles using titanium dioxide nanoparticles as light scatterers in the same group.[6b] These work light a hope of using CNPs as the gain medium to achieve lasing.

The strongest emission of CNPs were usually observed in deep blue or blue regions, which was supposed to arise from electron-hole recombination or quantum size effect (intrinsic state emission). In some cases, strong emission can be achieved in green region, ascribing to surface defects (defect state emission).[7] Surface defect states are in general energy dissipative, hard to support lasing emission. Thus, it is of great scientific interest, especially for understanding their luminescence mechanism and future applications in lasers and optoelectronic devices, to demonstrate the lasing capacities of CNPs in green region and to reveal the influence factors.

High photoluminescence (PL) quantum yield and low optical loss are important factors in achieving sufficient optical gain for lasing. Surface unfunctionalized CNPs usually exhibit weak luminescence (<5%). To achieve enhanced luminescence, amine- or hydroxyl-group enriched molecules have been used as surface passivation agents for CNPs.[6,8,9] Recently, PL quantum yields of CNPs with surface passivation up to 80% were reported in blue region by several groups.[9] However, it is still a challenge to modulate their optical properties and to achieve high PL quantum yield in green region.[7] Previously, we reported an easy, economic, and green one-step microwave synthesis for water-soluble luminescent CNPs from urea and citric acid (mass ratio 1:1), which displayed low toxicity to both plants and animals.[10] The CNPs aqueous solutions exhibit dual fluorescence bands (blue and green fluorescence bands) under UV excitation. In this work, we demonstrated that the optical properties of CNPs can be modified by the dopant-N atom and sp^2 C-contents. CNPs prepared with the low urea mass ratio of 0.2:1 (CNP1) exhibited blue emissions (maximum PL quantum yield: 15%). Increased dopant-N atom and sp^2 C-contents were observed in the CNPs prepared with high urea mass ratio of 2:1 (CNP2), which exhibited green emission (maximum PL quantum yield up to 36% in ethanol aqueous solution). Amplified spontaneous emission (ASE) was only observed in CNP2

Prof. S. Qu, Prof. X. Liu, Dr. X. Guo, Dr. M. Chu, Prof. L. Zhang, Prof. D. Shen
State Key Laboratory of Luminescence and Applications
Changchun Institute of Optics
Fine Mechanics and Physics
Chinese Academy of Sciences
Changchun, 130033, China
E-mail: liuxy@ciomp.ac.cn; dzshen824@sohu.com

DOI: 10.1002/adfm.201303352

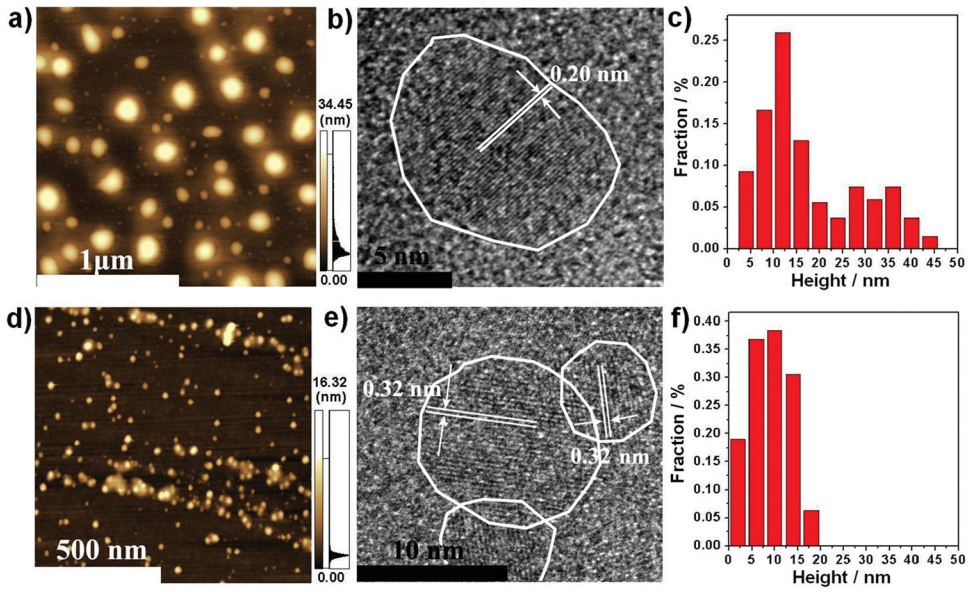

Figure 1. a) AFM, b) HRTEM images, and c) height distribution of CNP1; d) AFM, e) HRTEM images, and f) height distribution of CNP2. The shapes of CNPs in HRTEM images were outlined in white lines.

ethanol aqueous solution. Green lasing emission was realized from CNP2 ethanol aqueous solution (ethanol volume concentration: 65%) in a linear long Fabry-Perot cavity, indicating unequivocally that CNP2 can be used as a gain medium to achieve lasing. To the best of our knowledge, it is the first case of lasing emission of CNPs in green region.

2. Results

2.1. Preparation of CNP1 and CNP2

The microwave synthesis of CNPs followed procedures given in our previous work.[10] CNP1, and CNP2 were prepared from urea and citric acid in the mass ratios of 0.2:1, and 2:1, respectively. First, citric acid (3 g) and urea (0.6 g or 6 g) were added to distilled water (10 mL) to form a transparent solution. The solution was then heated in a domestic 650 W microwave oven for 4–5 mins, during which the solution changed from colorless liquid to brown and finally dark-brown clustered solid, indicating the formation of CNPs. This solid was then transferred to a vacuum oven and heated at 60 °C for 1 h. The as-prepared CNPs were processed in water or ethanol aqueous solution (ethanol volume concentration: 65%), followed by centrifugation (3000 r min^{-1}, 20 min) to remove large or agglomerated particles.

2.2. Characterization of CNP1 and CNP2

The morphologies of CNP1 and CNP2 were characterized using transmission electron microscopy (TEM) and atomic force microscopy (AFM). Drops of CNP1 or CNP2 dilute ethanol aqueous solution were deposited on carbon-coated copper grids for TEM and on silicon substrates for AFM. Morphology characterizations illustrated that CNP1 and CNP2 are spherical and well dispersed (**Figure 1**). The sizes of CNP1 were in the range from 4 to 45 nm, whereas for CNP2 the range is from 2 to 20 nm. Well-resolved lattice fringes with an interplanar spacing of 0.20 nm of CNP1 (Figure 1b) are close to the (100) facet of graphitic carbon.[11] Well-resolved lattice fringes with an interplanar spacing of 0.32 nm were observed in CNP2 (Figure 1e), which is consistent with the (002) lattice planes of graphitic carbon. The X-ray powder diffraction (XRD) patterns of the CNP1 (**Figure 2**a) display two broad peaks centered at 4.9 Å and 3.3 Å. In contrast, a strong diffraction (3.2 Å) was observed in XRD patterns of CNP2, which agree well with the HRTEM observation.

The chemical compositions of CNP1 and CNP2 were investigated. X-ray photoelectron spectroscopy (XPS) spectra of CNP1 and CNP2 show three peaks at 284.0, 400.0, and 530.6 eV (Figure 2b), which are attributed to C_{1s}, N_{1s}, and O_{1s}, respectively. The ratio of N atoms and C atoms in CNP1 from XPS results is about 0.17: 1 which is a little lower than that in CNP2 (0.19:1). It should be noted that CNP2 exhibits decreased O atoms content in contrast to CNP1 (**Table 1**). The C_{1s} spectrum of CNP1 shows five peaks at 284.5, 285.2, 285.7, 286.7, and 288.7 eV (Figure 2c) that are attributed to sp^2 C, sp^3 C, C–N, C–O, and C = N/C = O, respectively.[12] In contrast, the C_{1s} spectrum of CNP2 (Figure 2d) shows enhanced sp^2 C, indicating increased sp^2 C clusters. The N_{1s} spectrum of CNP1 shows three peaks at 399.8, 400.3, and 401.9 eV (Figure 2e), which are attributed to the C–N–C, N–(C)3, and N–H bands, respectively, indicating dopant-N atoms (C–N–C, N–(C)3) and amide-N (N–H).[13] In contrast, the N_{1s} spectrum of CNP2 shows increased dopant-N atoms content (Figure 2f, Table 1). Dopant-N atoms were further evidenced by the appearance of the C = N bond at 1566 cm^{-1} in the FT-IR spectrum (Figure S2, Supporting Information). The surface functional groups of CNP1 and CNP2 were detected using Fourier transform infrared

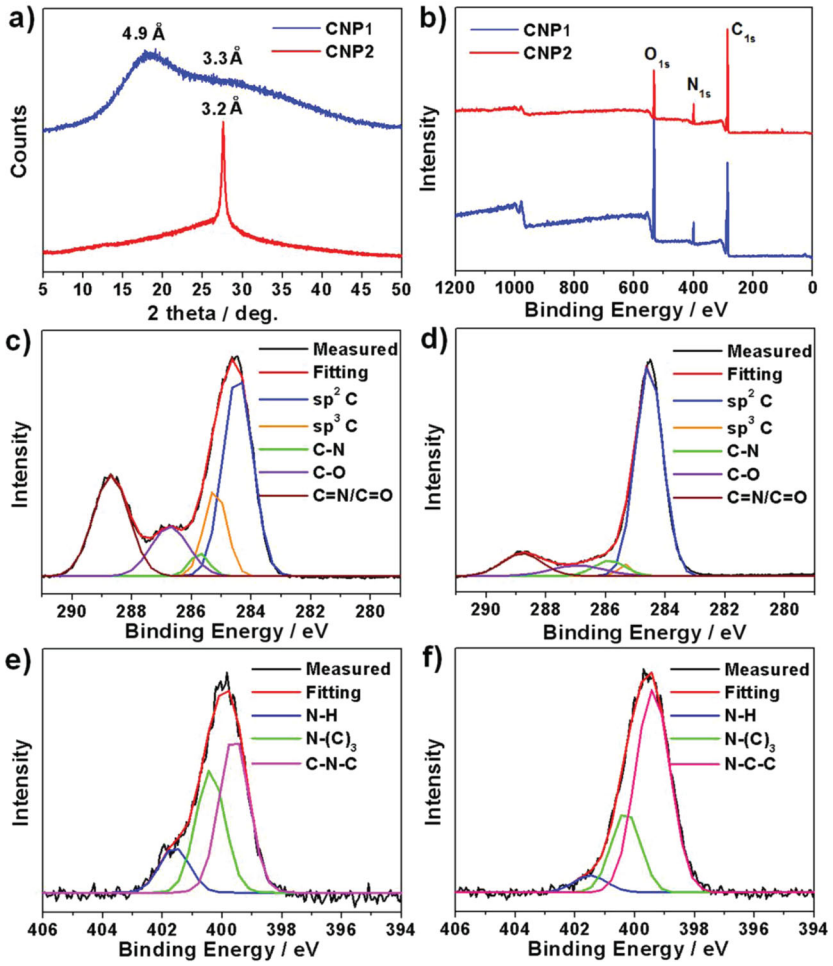

Figure 2. a) XRD patterns and b) XPS spectra of CNP1 and CNP2 in the dry state; c) C_{1s} and e) N_{1s} spectra of CNP1 in the dry state; d) C_{1s} and f) N_{1s} spectra of CNP2 in the dry state.

(FT-IR) (Figure S2, Supporting Information). Broad absorption bands at 3050–3552 cm^{-1} are assigned to ν(N-H) and ν(O-H). Absorption bands at 1640–1780 cm^{-1} are assigned to ν(C = O). These functional groups improve hydrophilicity and stability of the prepared CNPs in aqueous systems.

2.3. Optical Properties of CNP1 and CNP2

Broad absorption spectrum with an absorption band centered at 336 nm of CNP1 dilute aqueous solution indicates a π–π conjugated structure (Figure S3, Supporting Information). This solution has excitation-wavelength-dependent PL (Figure S5, Supporting Information). The strongest emission was observed centered at 440 nm under 360-nm excitation with a PL quantum yield of 15%. The luminescence decay of CNP1 dilute aqueous solution monitored at 440 nm under 360-nm excitation is mono-exponential with a lifetime of 9.0 ns (Figure S7, Supporting Information). By increasing the mass ratio of urea in the reactants, a long-wavelength absorption band appeared and the green emission bands were enhanced. The maximum absorption band of CNP2 aqueous solution was observed at 420 nm, indicating an extended π–π conjugated structure (Figure S3, Supporting Information). The CNP2 dilute aqueous solution exhibits also excitation-wavelength-dependent PL (Figure S6, Supporting Information). The strongest emission was observed centered at 540 nm under 420-nm excitation with PL quantum yield of 18%. The luminescence decay of CNP2 dilute aqueous solution monitored at 540 nm under 420-nm excitation is mono-exponential with a lifetime of 5.8 ns (Figure S8, Supporting Information). CNP1 and CNP2 dilute ethanol aqueous solutions exhibit blue-shifted emissions compared with their aqueous solutions (**Figure 3**). The strongest emission of CNP1 dilute ethanol aqueous solution was observed centered at 430 nm under 360-nm excitation. The strongest emission of CNP2 dilute ethanol aqueous solution was observed centered at 526 nm under 420-nm excitation. The PL quantum yield of CNP1 dilute ethanol aqueous solution is nearly unchanged, whereas for CNP2 dilute ethanol aqueous solution under 420-nm excitation, an enhanced PL quantum yield up to 36% was observed. The luminescence lifetime of CNP1 dilute ethanol aqueous solution monitored at 430 nm under 360-nm excitation is decreased to 8.1 ns (Figure S7, Supporting Information), while the luminescence lifetime of CNP2 dilute ethanol aqueous solution monitored at 526 nm under 420-nm excitation is increased to 10.2 ns (Figure S8, Supporting Information). It should be noted that the overlap between absorption and emissions of the CNP2 solutions is significantly smaller than that of the CNP1 solutions.

Table 1. Relative ratios of C_{1s}, N_{1s} and O_{1s} in CNP1 and CNP2 from XPS analysis results.

	C_{1s}	N_{1s}		O_{1s}	
		amide-N	dopant-N	C-O	C = O/COOH
CNP1	1	0.03	0.14	0.44	0.79
CNP2	1	0.01	0.18	0.11	0.44

2.4. Optical Pumping Investigations on CNP1 and CNP2

Optical pumping investigations on the prepared CNPs were carried out in their aqueous and ethanol-aqueous solutions at various concentrations. The pumping beam was a Nd:YAG laser beam (λ = 355 nm, pulse width 10 ns at a 1-Hz repetition rate) and focused by a cylindrical lens into a 0.4-mm-wide stripe. ASE was not observed in the prepared CNPs aqueous solutions or CNP1 ethanol aqueous solutions, but appeared

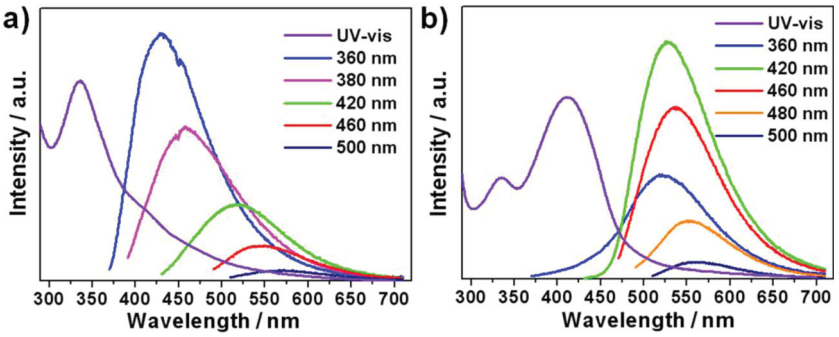

Figure 3. UV-Vis absorption and PL spectra of a) CNP1 dilute ethanol aqueous solution and b) CNP2 dilute ethanol aqueous solution.

in CNP2 ethanol aqueous solutions. The ASE threshold for CNP2 ethanol aqueous solution at 6 mg/mL is about 200 kW cm^{-2} (**Figure 4**b). Increasing the excitation power above the threshold, the intensity and full width at half maximum (FWHM) of the ASE spectra are greatly increased and further narrowed, respectively (Figure 4a,b; Supporting Information Figure S10). At the excitation power of 320 kW cm^{-2}, the ASE spectrum centered at 555 nm with FWHM of 64 nm. To realize laser-cavity resonance, mirrors were fabricated on two parallel plates of a quartz cuvette to form a linear long Fabry-Perot cavity (distance between the parallel mirrors is about 5 mm). The mirrors were distributed Bragg reflector (DBR) structures of 15 and 27 pairs of HfO_2/SiO_2 quarter-wave layers, respectively. The 15-pair-DBR (front mirror) shows average reflectance of 95.3% in 540–570 nm, and the 27-pair-DBR (back mirror) shows average reflectance of 99.5% in 540–570 nm (Figure 4c). The focused pumping laser stripe is vertical to the mirrors, as shown in **Figure 5**a. The dependence of the spectral peak intensity on pumping density indicates a clear laser threshold of about 60 kW cm^{-2} (Figure 4d), above which a sharp increase in output intensity was observed (Figure S11, Supporting Information). An operating CNP-based laser device exhibited a well-defined beam of bright green laser emissions in a direction orthogonal to the mirrors (see photo in Figure 5c). Figure 4d shows the output laser emission spectra at the excitation power of 274 kW cm^{-2}. The laser spectrum centered at 561 nm with the FWHM of 4 nm. The far-field profile of the output laser emission above the threshold is shown in Figure 4e. The measured far-field full divergence angle is less than 2 mrad. Furthermore, the output laser emission is polarized. The most intense emission was obtained when the polarization of the detection was set parallel to that of the laser. The maximal/minimal intensity ratio (I_{max}/I_{min}) as observed in Figure 4f is about 10. It is expected that there is fine structure from the lasing spectra because the Fabry-Perot cavity supports longitudinal modes. The mode spacing of the fine structure ($\Delta\lambda$) can be written as follows:

$$\Delta\lambda = \lambda^2/2nL \quad (1)$$

where $\lambda = 561$ nm the lasing wavelength, $n = 1.38$ the refractive index of CNP2 ethanol aqueous solution (6 mg mL^{-1}) in visible regions and $L = 5$ mm the length of cavity. The calculated $\Delta\lambda$ is around 0.02 nm. Due to the resolution limitation of our monochromator (0.08 nm), the high-resolution spectrum of the output laser at the excitation power of 274 kW cm^{-2} exhibits numerous peaks (inset) evenly spaced with 0.08 nm (Figure 4g). Each peak here should be an envelope of several resonant cavity modes, which is reasonable with long Fabry Perot cavity laser. These results unambiguously demonstrate that CNP2 ethanol aqueous solutions can be used as a gain medium to achieve lasing. Furthermore, CNP2 has superior photostability compared with C545T dye (a conventional green laser dye). The irradiating source was a laser beam ($\lambda = 355$ nm, pulse width 1 ns, 200-Hz repetition rate, 75 μJ output) from a FTSS 355–50 (Crylas, Berlin Germany). The emission of C545T ethanol solution (0.1 mg mL^{-1}) was quickly quenched after ten minutes laser irradiation from severe photobleaching (Figure 4h). In contrast, the CNP2 ethanol aqueous solution (0.1 mg mL^{-1}) preserved approximately 60% of the original PL intensity after ten minutes laser irradiation.

3. Discussion

We also prepared CNPs (CNP0) from citric acid without adding urea in the same synthesis process. CNP0 aqueous solution showed weak luminescence. The strongest emission was observed centered at 475 nm under 380-nm excitation (Figure S4, Supporting Information) with a PL quantum yield of 3%, similar to reports of other groups.[8g] It was previously reported that the doped nitrogen could enhance the emission of the CNPs by inducing an upward shift of the Fermi level and electrons in the conduction band.[14] Urea in the reactants acted as nitrogen doping sources to acheive enhanced PL quantum yields of CNP1 and CNP2 compared with CNP0.

Considering the bandgap-like absorptions and the presence of sp^2 C, the absorption in the CNPs might originate from the sp^2 clusters, which behave as absorption centers.[15] Recently, Chen et al. proposed that small sp^2 clusters with sufficiently large gaps are responsible for the blue luminescence observed in graphene oxide.[16] Pan et al. proposed that the blue luminescence is due to small sp^2 clusters embedded in CNPs.[17] Thus, the embedded small sp^2 clusters in CNP1 could account for the absorption in UV region and the blue luminescence. The increased sp^2 C clusters in CNP2, as demonstrated by XPS results, indicated extended conjugated structures compared with CNP1, which could lead to long-wavelength absorptions and emissions, agreeing well with their absorption and PL spectra. It can be concluded that the absorption and emission of as-prepared CNPs can be modulated by the dopant-N atom and sp^2 C-contents. Seo and Cho et al. pointed out that the green luminescence from grapheme oxide quantum dots originates from defect states with oxygenous functional groups.[7a] In our system, the contents of oxygenous functional groups (C–O and C = O/COO) on CNP2 were much less than that of CNP1 as evidenced by XPS analysis results (Table **1**). The green emission from CNP2 can not be ascribed to defect states with oxygenous functional groups. Considering ASE and lasing

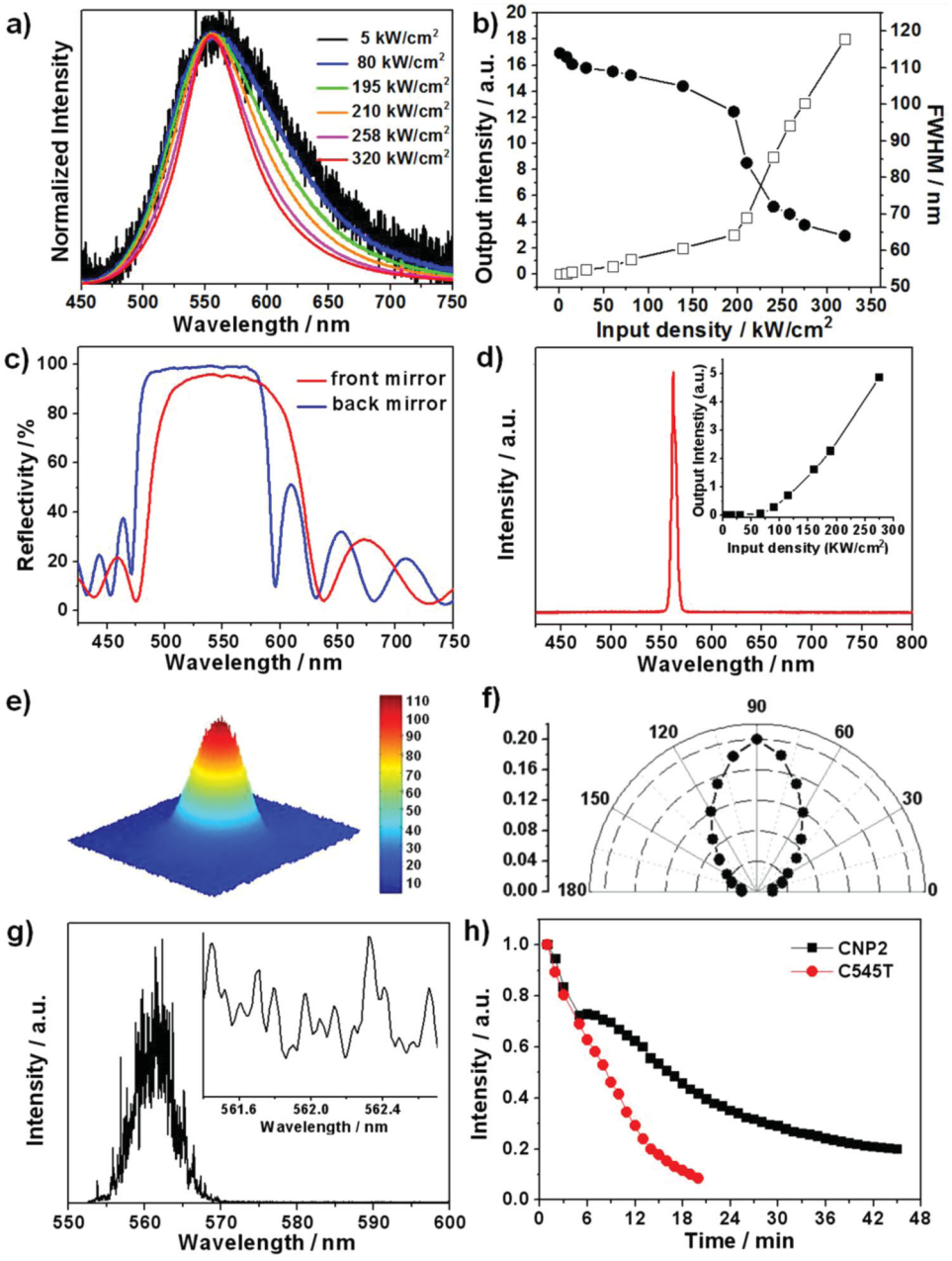

Figure 4. a) Normalized emission spectra of CNP2 ethanol aqueous solution (6 mg mL^{-1}) under various optically pumped pulse densities. b) Pumping density dependence of output peak intensity (□) and FWHM value (•) of CNP2 ethanol aqueous solution (6 mg m^{-1}). c) Measured reflectance spectra of the fabricated mirrors on a cuvette. d) Emission spectra of the operating CNP-based laser device at the excitation power of 274 kW cm^{-2} (inset shows the dependence of the spectral peak intensity on the pumping density). e) Far-field output beam profile at the excitation power of 274 kW cm^{-2}. f) Relationship between the emission intensity and the polarization angle at the excitation power of 274 kW cm^{-2} (angle between collection polarizer and the pumping laser beam). g) High-resolution emission spectra of the operating CNP-based laser device at the excitation power of 274 kW cm^{-2} (inset shows a portion of the same spectrum under higher resolution). h) Plots of PL intensity of C545T ethanol solution (0.1 mg mL^{-1}) and CNP2 ethanol solution (0.1 mg mL^{-1}) versus irradiation time under a laser beam irradiation (λ = 355 nm, pulse width 1 ns, 200-Hz repetition rate, 75 μJ output) at room temperature.

emission from CNP2, we propose that the green emission from CNP2 is attributed to electron-hole recombination (intrinsic state emission).

The overlap between absorption and emission of CNP1 solutions is relatively large, causing great loss in the resonator cavity due to reabsorption/reemission phenomena and it is hard to support lasing emission. In contrast, the overlap between absorption and emission of the CNP2 solutions is much smaller than that of the CNP1 solutions. ASE and lasing emission appeared only in CNP2 ethanol aqueous solutions, which exhibited enhanced PL quantum yield compared with its aqueous solutions. Based on the results above, it can be

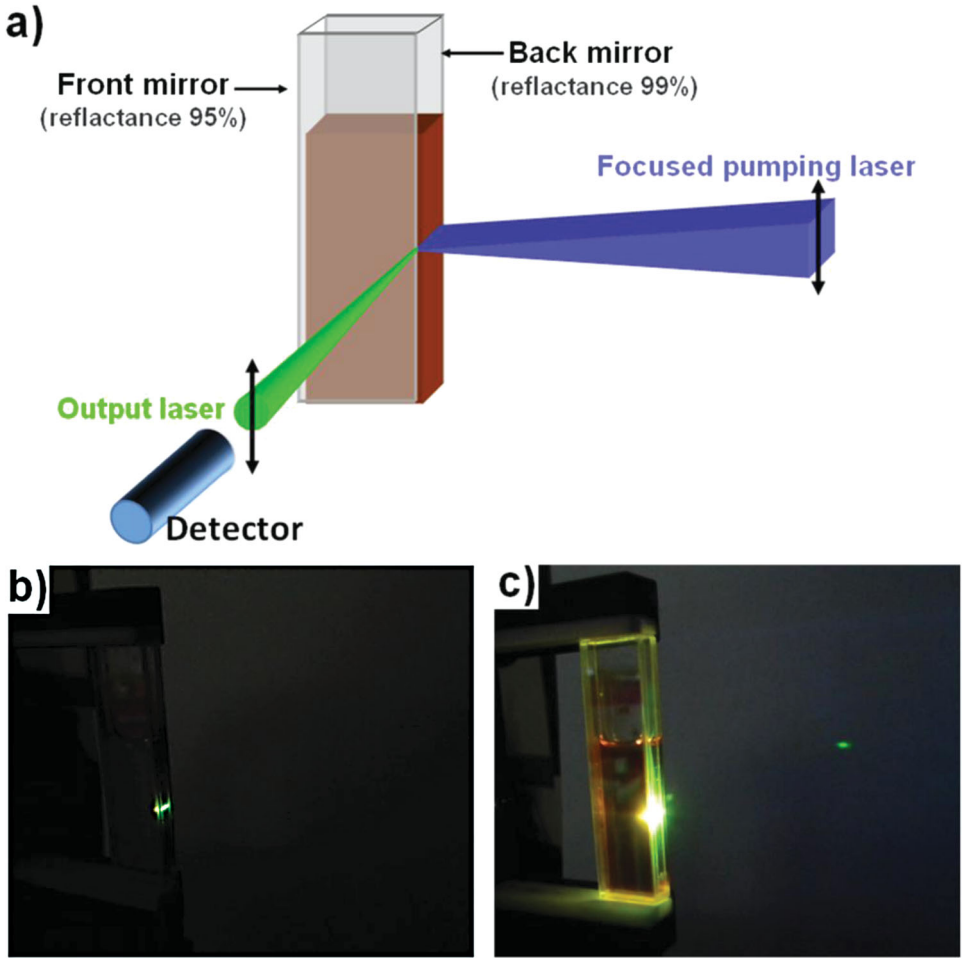

Figure 5. a) Schematic diagram of experimental setup for optical pumping investigations of the CNP-based laser device (the black double arrows illustrate polarizations of the pumpping laser and output laser). Photos of the operating CNP-based laser device under 355 nm laser pumping at b) 30 kW cm^{-2} and c) 190 kW cm^{-2}.

concluded that the high PL quantum yield and small overlap between absorption and emissions of CNP2 ethanol aqueous solution are the key factors in achieving lasing emission.

4. Conclusions

In conclusion, we have demonstrated that the optical properties of CNPs can be modulated by the dopant-N atom and sp^2 C-contents. CNPs prepared with low urea mass ratio of 0.2:1 (CNP1) exhibited blue emission (maximum PL quantum yield: 15%). Increased dopant-N atom and sp^2 C-contents were observed in CNPs prepared with high urea mass ratio of 2:1 (CNP2), which exhibit green emissions (maximum PL quantum yield up to 36% in ethanol aqueous solution). ASE was only observed in CNP2 ethanol aqueous solution. Green lasing emission was achieved from CNP2 ethanol aqueous solution in a linear long Fabry-Perot cavity, indicating CNP2 has potential of a gain medium to achieve lasing. CNP2 is superior in photostability compared with C545T dye. The green emission from CNP2 is speculated to be attributed to electron-hole recombination (intrinsic state emission). The high PL quantum yield and small overlap between absorption and emission of CNP2 ethanol aqueous solution are the key factors in achieving lasing emission. We expect our endeavor may raise attentions on the lasing phenomena of the environment-friendly CNPs and be benefit for understanding their luminescence mechanism.

5. Experimental Section

Experimental Materials: Citric acid, urea, and ethanol were purchased from Beijing Chemical Corp. HfO_2 and SiO_2 were purchased from Beijing General Research Institute for Nonferrous Metals. C545T was purchased from Beijing Elight Corp. All chemicals were used as received without further purification. The water used in all experiments was purified with a Millipore system.

Preparation of Mirrors: Parallel mirrors were fabricated on a quartz cuvette. The HfO_2 and SiO_2 layers were deposited by electron beam evaporation at a substrate temperature of 250 °C in an oxygen pressure of 2×10^{-2} Pa.

Characterizations: TEM observations were performed on a FEI Tecnai-G2-F20 TEM at 200 kV. AFM measurements were performed on a SA400HV with a Seiko SPI3800N controller. Energy dispersive

X-ray (EDX) analysis was performed by a EDAX Genesis 2000 Energy Dispersive Spectroscopy. Raman spectra were collected using an UV-lamp spectroscope with a 300 mW Ar+ laser (488 nm) as the excitation source. PL spectra were collected using a FLS920 spectrometer and UV-visible absorption spectra were recorded on a Shimadzu UV-3101PC spectrophotometer. Photoluminescence quantum yields were obtained in a calibrated integrating sphere in FLS920 spectrometer. Fluorescence lifetimes were measured using FLS920 time-corrected single photon counting system. XPS analyzes were measured on an ESCALAB MK II X-ray photoelectron spectrometer using Mg as the exciting source. FT-IR spectrum was recorded with a Perkin–Elmer spectrometer (Spectrum One B). XRD was performed with a Bruker Advance D8 X-ray diffractometer. Optical pumping investigations were performed using a Nd:YAG laser with a repetition rate of 1 Hz and pulse duration of about 10 ns. The emission spectra were obtained using an Ocean Optics Maya2000 Pro Fiber Optic Spectrometer and AvaSpec Multichannel Fiber Optic Spectrometer. The laser power was recorded using a Newport 2936C laser power meter.

Supporting Information

Supporting Information is available from the Wiley Online Library or from the author.

Acknowledgements

This work is supported by the CAS Innovation Program, National Science Foundation of China No. 51103144, 61106057, 51102228, 61274126, and Project supported by State Key Laboratory of Luminescence and Applications.

Received: September 28, 2013
Revised: November 12, 2013
Published online: December 27, 2013

[1] a) S. N. Baker, G. A. Baker, *Angew. Chem. Int. Ed.* **2010**, *49*, 6726; b) J. C. G. Esteves da Silva, H. M. R. Goncalves, *Trends Anal. Chem.* **2011**, *30*, 1327; c) H. Li, Z. Kang, Y. Liu, S. T. Lee, *J. Mater. Chem.* **2012**, *22*, 24230.

[2] a) L. Cao, X. Wang, M. J. Meziani, F. Lu, H. Wang, P. G. Luo, Y. Lin, B. A. Harruff, L. M. Veca, D. Murray, S. Y. Xie, Y. P. Sun, *J. Am. Chem. Soc.* **2007**, *129*, 11318; b) F. Wang, Z. Xie, H. Zhang, C. Y. Liu, Y. G. Zhang, *Adv. Funct. Mater.* **2011**, *21*, 1027; c) Y. Xu, M. Wu, Y. Liu, X. Z. Feng, X. B. Yin, X. W. He, Y. K. Zhang, *Chem. Eur. J.* **2013**, *19*, 2276.

[3] a) L. Cao, S. Sahu, P. Anilkumar, C. E. Bunker, J. Xu, K. A. S. Fernando, P. Wang, E. A. Guliants, K. N. Tackett, Y. P. Sun, *J. Am. Chem. Soc.* **2011**, *133*, 4754; b) H. T. Li, X. He, Z. Kang, H. Huang, Y. Liu, J. Liu, S. Lian, A. C. H. Tsang, X. Yang, S. T. Lee, *Angew. Chem. Int. Ed.* **2010**, *49*, 4430.

[4] a) H. X. Zhao, L. Q. Liu, Z. D. Liu, Y. Wang, X. J. Zhao, C. Z. Huang, *Chem. Commun.* **2011**, *47*, 2604; b) Wei, C. Xu, J. Ren, B. Xu, X. Qu, *Chem. Commun.* **2012**, *48*, 1284; c) L. Zhou, Y. Lin, Z. Huang, J. Ren, X. Qu, *Chem. Commun.* **2012**, *48*, 1147; d) S. Liu, J. Tian, L. Wang, Y. Zhang, X. Qin, Y. Luo, A. M. Asiri, A. O. Al-Youbi, X. Sun, *Adv. Mater.* **2012**, *24*, 2037; e) M. J. Krysmann, A. Kelarakis, P. Dallas, E. P. Giannelis, *J. Am. Chem. Soc.* **2012**, *134*, 747; f) J. M. Liu, L. Lin, X. X. Wang, S. L. Lin, W. L. Cai, L. H. Zhang, Z. Y. Zheng, *Analyst* **2012**, *137*, 2637; g) W. Shi, X. Li, H. Ma, *Angew. Chem. Int. Ed.* **2012**, *51*, 6432; h) A. Zhu, Q. Qu, X. Shao, B. Kong, Y. Tian, *Angew. Chem. Int. Ed.* **2012**, *51*, 7185.

[5] a) X. Yan, X. Cui, B. Li, L. Li, *Nano Lett.* **2010**, *10*, 1869; b) Y. Li, Y. Hu, Y. Zhao, G. Shi, L. Deng, Y. Hou, L. Qu, *Adv. Mater.* **2011**, *23*, 776.

[6] a) W. F. Zhang, H. Zhu, S. F. Yu, H. Y. Yang, *Adv. Mater.* **2012**, *24*, 2263; b) H. Zhu, W. Zhang, S. F. Yu, *Nanoscale* **2013**, *5*, 1797.

[7] a) F. Liu, M.-H. Jang, H. D. Ha, J.-H. Kim, Y.-H. Cho, T. S. Seo, *Adv. Mater.* **2013**, *25*, 3657; b) S. Zhu, J. Zhang, S. Tang, C. Qiao, L. Wang, H. Wang, X. Liu, B. Li, Y. Li, W. Yu, X. Wang, H. Sun, B. Yang, *Adv. Funct. Mater.* **2012**, *22*, 4732; c) H. Zheng, Q. Wang, Y. Long, H. Zhang, X. Huang, R. Zhu, *Chem. Commun.* **2011**, *47*, 10650.

[8] a) X. Wang, L. Cao, S. T. Yang, F. Lu, M. J. Meziani, L. Tian, K. W. Sun, M. A. Bloodgood, Y. P. Sun, *Angew. Chem. Int. Ed.* **2010**, *49*, 5310; b) Y. P. Sun, B. Zhou, Y. Lin, W. Wang, K. A. S. Fernando, P. Pathak, M. J. Meziani, B. A. Harruff, X. Wang, H. F. Wang, P. J. G. Luo, H. Yang, M. E. Kose, B. L. Chen, L. M. Veca, S. Y. Xie, *J. Am. Chem. Soc.* **2006**, *128*, 7756; c) H. Zhu, X. Wang, Y. Li, Z. Wang, F. Yang, X. Yang, *Chem. Commun.* **2009**, 5118; d) C. Fowley, B. McCaughan, A. Devlin, I. Yildiz, F. M. Raymo, J. F. Callan, *Chem. Commun.* **2012**, *48*, 9361; e) A. B. Bourlinos, A. Stassinopoulos, D. Anglos, R. Zboril, V. Georgakilas, E. P. Giannelis, *Chem. Mater.* **2008**, *20*, 4539; f) A. B. Bourlinos, R. Zbořil, J. Petr, A. Bakandritsos, M. Krysmann, E. P. Giannelis, *Chem. Mater.* **2012**, *24*, 6; g) X. Zhai, P. Zhang, C. Liu, T. Bai, W. Li, L. Dai, W. Liu, *Chem. Commun.* **2012**, *48*, 7995; h) P. Zhang, W. Li, X. Zhai, C. Liu, L. Dai, W. Liu, *Chem. Commun.* **2012**, *48*, 10431; i) P. C. Hsu, H. T. Chang, *Chem. Commun.* **2012**, *48*, 3984; j) F. Wang, Z. Xie, H. Zhang, C. Liu, Y. Zhang, *Adv. Funct. Mater.* **2011**, *21*, 1027; k) H. Tetsuka, R. Asahi, A. Nagoya, K. Okamoto, I. Tajima, R. Ohta, A. Okamoto, *Adv. Mater.* **2012**, *24*, 5333; l) P. C. Chen, Y. N. Chen, P. C. Hsu, C. C. Shih, H. T. Chang, *Chem. Commun.* **2013**, *49*, 1639.

[9] a) Z. Xie, F. Wang, C. Liu, *Adv. Mater.* **2012**, *24*, 1716; b) S. Zhu, Q. Meng, L. Wang, J. Zhang, Y. Song, H. Jin, K. Zhang, H. Sun, H. Wang, B. Yang, *Angew. Chem. Int. Ed.* **2013**, *52*, 3953.

[10] a) S. Qu, X. Wang, Q. Lu, X. Liu, L. Wang, *Angew. Chem. Int. Ed.* **2012**, *51*, 12215; b) S. Qu, H. Chen, X. Zheng, J. Cao, X. Liu, *Nanoscale* **2013**, *5*, 5514.

[11] J. Wang, C.-F. Wang, S. Chen, *Angew. Chem. Int. Ed.* **2012**, *51*, 9297.

[12] L. Li, J. Ji, R. Fei, C. Wang, Q. Lu, J. Zhang, L. Jiang, J. Zhu, *Adv. Funct. Mater.* **2012**, *22*, 2971.

[13] S. Fleutot, J.-C. Dupin, G. Renaudin, H. Martinez, *Phys. Chem. Chem. Phys.* **2011**, *13*, 17564.

[14] P. Ayala, R. Arenal, A. Loiseau, A. Rubio, T. Pichler, *Rev. Mod. Phys.* **2010**, *82*, 1843.

[15] T. Heitz, C. Godet, J. G. Boureé, B. Drevillon, J. P. Conde, *Phys. Rev. B* **1999**, *60*, 6045.

[16] G. Eda, Y. Y. Lin, C. Mattevi, H. Yamaguchi, H. A. Chen, I. S. Chen, C. W. Chen, M. Chhowalla, *Adv. Mater.* **2010**, *22*, 505.

[17] D. Pan, J. Zhang, Z. Li, C. Wu, X. Yana, M. Wu, *Chem. Commun.* **2010**, *46*, 3681.